arXiv:hep-lat/0304010v1 16 Apr 2003

Thermal Width Broadening of the 0^{++} Glueball Spectrum near T_c

Noriyoshi Ishii[1], Hideo Suganuma[2], and Hideo Matsufuru[3]

[1]*Radiation Laboratory, RIKEN (The Institute of Physical and Chemical Research), 2–1 Hirosawa, Wako, Saitama 351–0198, Japan*
[2]*Faculty of Science, Tokyo Institute of Technology, 2–12–1 Ohkayama, Meguro, Tokyo 152–8552, Japan*
[3]*Yukawa Institute for Theoretical Physics, Kyoto University, Kitashirakawa-Oiwake, Sakyo, Kyoto 606–8502, Japan*

We study the 0^{++} glueball correlator constructed with SU(3) anisotropic quenched lattice QCD at various temperature taking into account the possible existence of the thermal width in the ground-state peak. For this purpose, we adopt the Breit-Wigner ansatz, analysing the lattice data obtained with 5,500–9,900 gauge configurations at each T. The results indicate the significant thermal width broadening as $\Gamma(T_c) \sim 300$ MeV with a reduction in the peak center as $\Delta\omega_0(T_c) \sim 100$ MeV in the vicinity of the critical temperature T_c.

§1. Introduction

At finite temperature/density, QCD changes its vacuum structure such as the reduction of the string tension, the partial chiral restoration, etc, even below the critical temperature T_c of the QCD phase transition. These changes are expected to affect the hadrons leading to the changes in the various hadronic properties, since hadrons are composite particles consisting of quarks and gluons. The hadronic pole-mass shifts are thus considered to serve as the important precritical phenomena of the QCD phase transition near the critical temperature T_c, and have been extensively studied by using various QCD-motivated low-energy effective theories.1),2),3),4) These studies suggest the pole-mass reductions of charmoniums, light $q\bar{q}$ mesons and the glueball near the critical temperature.

As for the lattice QCD, it has been more popular to study the spatial correlations (the screening mass) than the temporal correlations (the pole-mass) at finite temperature. This is because the temporal extension of the lattice is subject to $1/T$. Accordingly, number of the temporal lattice data decreases at finite temperature, which used to be the main obstacle for the lattice QCD to measure the hadronic pole-mass. Recently, by using the anisotropic lattice, which has a finer lattice spacing in the temporal direction than in the spatial direction, the accurate measurement of the pole-mass with the lattice QCD has become possible at finite temperature.5),6) Quenched-level Monte Carlo calculations reveal the profound results that the pole-masses of the $q\bar{q}$ mesons are almost unchanged from their zero-temperature values in the confinement phase,6),7) while the pole-mass of the 0^{++} glueball shows the 300 MeV reduction near the critical temperature.8) Although these thermal effects are weaker than anticipated by the effective model studies, these tendencies are consistent with the recent quenched-level lattice studies on the screening mass at finite temperature.[9),10)] In these analysis, the bound-state peaks in the spectral function are assumed to be narrow enough. However, at finite temperature, each bound-state acquires the thermal width through the interaction with the heat bath. The thermal width is expected to grow up with temperature, which may lead to a possible collapse of the narrow-peak assumption in some cases. In this paper, we first discuss what is the expected consequence of the thermal width broadening. Then, we propose the Breit-Wigner ansatz for the fit-function for the temporal correlator at finite temperature. We finally show the results of the Breit-Wigner analysis of the 0^{++} glueball correlator at finite temperature.[11)]

§2. The Breit-Wigner Ansatz

We begin by considering the temporal correlator $G(\tau) \equiv Z(\beta)^{-1}\mathrm{Tr}\left(e^{-\beta H}\phi(\tau)\phi(0)\right)$ and its spectral representation as

$$G(\tau) = \int_{-\infty}^{\infty} \frac{d\omega}{2\pi} \frac{\cosh\left(\omega(\beta/2-\tau)\right)}{2\sinh(\beta\omega/2)} \rho(\omega), \tag{2·1}$$

where H denotes the QCD Hamiltonian, $Z(\beta) \equiv \mathrm{Tr}(e^{-\beta H})$ the partition function, $\phi(\tau)$ is the zero-momentum projected glueball operator[8)] represented in the imaginary-time Heisenberg picture as $\phi(\tau) \equiv e^{\tau H}\phi(0)e^{-\tau H}$. Here, $\rho(\omega)$ denotes the spectral function

$$\rho(\omega) \equiv \sum_{m,n} \frac{|\langle n|\phi|m\rangle|^2}{Z(\beta)} e^{-\beta E_m} \times 2\pi \left(\delta(\omega - \mathit{\Delta} E_{nm}) - \delta(\omega + \mathit{\Delta} E_{mn})\right), \tag{2·2}$$

where E_n denotes the energy of nth excited states, and $\mathit{\Delta} E_{mn} \equiv E_m - E_n$. Note that $\rho(\omega)$ is odd in ω reflecting the bosonic nature of the glueball. By adopting the appropriate ansatz for $\rho(\omega)$, we can extract various physical quantities such as the pole-mass and the width through the spectral representation Eq. (2·1).

We first consider the case where the bound-state peak is narrow.[6),7),8)] In this case, by introducing the temperature-dependent pole-mass $m(T)$, $\rho(\omega)$ can be parameterized as

$$\rho(\omega) \simeq 2\pi A \left(\delta(\omega - m(T)) - \delta(\omega + m(T))\right), \tag{2·3}$$

where A represents the strength. The second delta-function is introduced to respect the odd-function nature of $\rho(\omega)$. Since the corresponding $G(\tau)$ reduces to a single hyperbolic cosine, the pole-mass measurement at finite temperature can be performed in the same way as the standard mass measurement at zero temperature.[12)]

We next consider the case where the thermal width is wide. In this case, the peak center ω_0 of $\rho(\omega)$ represents the observed "mass" of the thermal hadron. What follows the narrow-peak assumption in this case ? To consider this, we notice that $G(\tau)$ can be thought of as a weighted average of hyperbolic cosines with the weight as

$$W(\omega) \equiv \frac{\rho(\omega)}{2\sinh(\beta\omega/2)}. \tag{2·4}$$

Here, $2\sinh(\beta\omega/2)$ in the denominator works as a biased factor, which enhances the smaller ω region while suppressing the larger ω region. Consequently, the pole-mass $m(T)$, which is approximated with the peak position of $W(\omega)$, is smaller than the peak center ω_0 of the spectral function $\rho(\omega)$, i.e., the observed hadron "mass".[11] What is the appropriate functional form of the fit-function ? To find this, we consider the retarded Green function $G_{\rm R}(\omega)$. At $T=0$, bound-state poles of $G_{\rm R}(\omega)$ are located on the real ω-axis. At $T>0$, bound-state poles are moving into the complex ω-plane with increasing temperature. Suppose that a bound-state pole is located at $\omega=\omega_0-i\Gamma$ as

$$G_{\rm R}(\omega)=\frac{A}{\omega-\omega_0+i\Gamma}+\cdots, \tag{2·5}$$

where A represents the residue at the pole, and "$\cdots$" the non-singular terms around the pole. Since the spectral function is the imaginary part of the retarded Green function, the contribution of this complex pole is expressed in the form of Lorentzian as

$$\begin{aligned}\rho(\omega)&=-2{\rm Im}\Big(G_{\rm R}(\omega)\Big). \\ &\simeq 2\pi A\Big(\delta_\Gamma(\omega-\omega_0)-\delta_\Gamma(\omega+\omega_0)\Big),\end{aligned} \tag{2·6}$$

where $\delta_\epsilon(x)\equiv\frac{1}{\pi}{\rm Im}\left(\frac{1}{x-i\epsilon}\right)=\frac{1}{\pi}\frac{\epsilon}{x^2+\epsilon^2}$ is a smeared delta-function with the width $\epsilon>0$. The second term in Eq. (2·6) is introduced to respect the odd-function nature of $\rho(\omega)$. In the limit $\Gamma\to+0$, Eq. (2·6) reduces to Eq. (2·3). We thus see that the appropriate fit-function, which takes into account the effect of the non-zero thermal width, is the following Breit-Wigner type as

$$g(\tau)\equiv\int_{-\infty}^{\infty}\frac{d\omega}{2\pi}\frac{\cosh\left(\omega(\beta/2-\tau)\right)}{2\sinh(\beta\omega/2)}\times 2\pi\widetilde{A}\Big(\delta_\Gamma(\omega-\omega_0)-\delta_\Gamma(\omega+\omega_0)\Big), \tag{2·7}$$

where $\widetilde{A}$, Γ and ω_0 are understood as fit-parameters, corresponding to the residue, the thermal width and the peak center, respectively. Note that $g(\tau)$ is a generalization of the ordinary single hyperbolic cosine fit-function. In order to use Eqs.(2·3) and (2·6), it is essential to suppress the higher spectral contributions. This is usually achieved by appropriate choices of the fit-ranges and also by improving the glueball operator, for instance, with the smearing method.[11]

§3. Numerical Result

We use the SU(3) anisotropic lattice plaquette action as

$$S_{\rm G}=\frac{\beta_{\rm lat}}{N_c}\frac{1}{\gamma_{\rm G}}\sum_{s,i<j\le 3}{\rm ReTr}(1-P_{ij}(s))+\frac{\beta_{\rm lat}}{N_c}\gamma_{\rm G}\sum_{i,j\le 3}{\rm ReTr}(1-P_{i4}(s)), \tag{3·1}$$

where $P_{\mu\nu}(s)\in{\rm SU}(3)$ denotes the plaquette operator in the μ-ν-plane. The lattice parameter and the bare anisotropic parameter are fixed as $\beta_{\rm lat}\equiv 2N_c/g^2=6.25$ and

$\gamma_G = 3.2552$, respectively, so as to reproduce renormalized anisotropy $\xi \equiv a_s/a_t = 4$.[5),6)] These parameter set reproduces $a_s^{-1} = 2.341(16)$ GeV and $a_t^{-1} = 9.365(66)$ GeV, where the scale unit is introduced from the on-axis data of the static inter-quark potential with the string tension $\sqrt{\sigma} = 440$ MeV. Numerical calculations are performed on the lattice of the size $20^3 \times N_t$ with various N_t. The critical temperature T_c on this lattice is estimated from the behavior of the Polyakov-loop susceptibility as $T_c \simeq 280$ MeV. The pseudo-heat-bath algorithm is adopted for the update of the gauge configurations. In order to construct the temporal glueball correlators, we use 5,500 to 9,900 gauge configurations. The statistical data are divided into bins of the size 100 to reduce the possible auto-correlations near the critical temperature. The smearing method is used to obtain the improved glueball operator, which is determined by examining its behavior at the lowest temperature, i.e., $T = 130$ MeV.

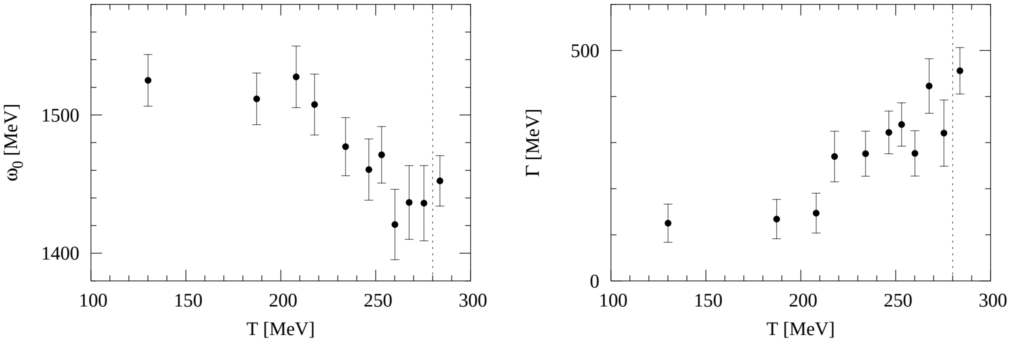

Fig. 1. The center ω_0 and the thermal width Γ of the lowest 0^{++} glueball peak plotted against temperature T. The vertical dotted lines indicate the critical temperature $T_c \simeq 280$ MeV.

The peak center and the thermal width of thermal glueball are obtained by the best-fit analysis of the suitably smeared glueball correlator $G(\tau)/G(0)$ with Eq. (2·7) at various temperatures. In Fig.1, the peak center ω_0 and the thermal width Γ are plotted against temperature. While narrow-peak ansatz leads to the pole-mass reduction of 300 MeV near T_c in Ref.,[8)] the Breit-Wigner analysis indicates a small reduction in the peak center as $\Delta\omega_0(T_c) \sim 100$ MeV. Instead, we observe a significant thermal width broadening as $\Gamma(T_c) \sim 300$ MeV.

§4. Summary and Discussion

We have studied the temporal correlator of the 0^{++} glueball at finite temperature using SU(3) anisotropic lattice QCD at quenched level with 5,500 to 9,900 gauge configurations at each temperature. We have proposed the Breit-Wigner ansatz for the fit-function to take into account the effect of the non-zero thermal width at finite temperature. We have applied the Breit-Wigner analysis to the temporal glueball correlator at finite temperature, and have observed a significant broadening of the thermal width as $\Gamma(T_c) \sim 300$ MeV with a slight reduction of the peak center as $\Delta\omega_0(T_c) \sim 100$ MeV in the vicinity of the critical temperature T_c.

In our present analysis, the Breit-Wigner ansatz seems to be the most appropriate one. Above T_c, however, the particle spectrum is expected to change drastically, and a proper assumption on the spectral function becomes less trivial. In this respect, it is interesting to apply the recently developed maximum entropy method (MEM),$^{13),14)}$ which requires no assumption on the shape of the spectral function.

Comparing our results$^{8),11)}$ with the related lattice QCD results,$^{6),7)}$ the quenched lattice QCD indicates that no significant thermal effects on the pole-mass have been so far observed in the $q\bar{q}$ sector,$^{6),7)}$ whereas a significant thermal effects can be observed in the glueball sector. These behaviors are consistent with the thermal effects on the screening mass.$^{9),10)}$

To discuss the experimental observability, it is important to estimate the effects of the dynamical quarks. One of the most significant contributions of the light dynamical quarks in unquenched QCD is the "string breaking" phenomenon, i.e., the light dynamical quark screens the colored flux and the long flux tubes are expected to be broken into pieces. The string breaking thus affects the long distance behavior of the inter-particle interactions, which could lead to a possible changes in the structures of hadrons in quenched QCD. In the case of the 0^{++} glueball, since its size is known to be rather compact as $R \simeq 0.4$ fm,$^{8),11)}$ such changes of the glueball structure is expected to be less significant. As for the mixing effect with the 0^{++} $q\bar{q}$ mesons in unquenched QCD, a recent unquenched lattice QCD study shows that there is no quark mass dependence on the glueball mass, which suggests that the mixing is actually rather small. However, it is in principle desirable to estimate the size of this mixing explicitly, which is left for the future studies.

Acknowledgments

The lattice QCD Monte Carlo calculations have been performed partly on NEC-SX5 at Osaka University and partly on HITACHI SR8000 at KEK.

References

1) T. Hatsuda, and T. Kunihiro, Phys. Rev. Lett. **55** (1985), 158.
2) T. Hashimoto, K. Hirose, T. Kinki, and O. Miyamura, Phys. Rev. Lett. **57** (1986), 2123.
3) T. Hatsuda, Y. Koike, and S.-H. Lee , Phys. Rev. D **47** (1993), 1225.
4) H. Ichie, H. Suganuma, and H. Toki, Phys. Rev. D **52** (1995), 2944.
5) T. R. Klassen, Nucl. Phys. B **533** (1998), 557.
6) QCD-Taro Collaboration, P. de Forcrand, Phys. Rev. D **63** (2001), 054501.
7) T. Umeda, R. Katayama, O. Miyamura, and H. Matsufuru, Int. J. Mod. Phys. **A16** (2001), 2215.
8) N. Ishii, H. Suganuma, and H. Matsufuru, Phys. Rev. D **66** (2002), 014507.
9) E. Laermann, and P. Schmidt, Eur. Phys. J. **C20** (2001), 541.
10) S. Datta, and S. Gupta, hep-lat/0208001.
11) N. Ishii, H. Suganuma, and H. Matsufuru, Phys. Rev. D **66** (2002), 094506.
12) C. J. Morningstar, and M. Peardon, Phys. Rev. D **66** (1999), 034509. and references therein.
13) M. Asakawa, T. Hatsuda, and Y. Nakahara, Prog. Part. Nucl. Phys. **46** (2001), 459.
14) M. Asakawa, T. Hatsuda, and Y. Nakahara, hep-lat/0208059.
15) A. Hart, and M. Teper, Phys. Rev. D **65** (2002), 034502.